HAL
archives-ouvertes.fr

A posteriori global error estimator based on the error in the constitutive relation for reduced basis approximation of parametrized linear elastic problems

Laurent Gallimard, David Ryckelynck

▶ To cite this version:

Laurent Gallimard, David Ryckelynck. A posteriori global error estimator based on the error in the constitutive relation for reduced basis approximation of parametrized linear elastic problems. Applied Mathematical Modelling, Elsevier, 2016, 40, pp.4271-4284. 10.1016/j.apm.2015.11.016 . hal-01305736

HAL Id: hal-01305736
https://hal-mines-paristech.archives-ouvertes.fr/hal-01305736

Submitted on 22 Jan 2018

HAL is a multi-disciplinary open access archive for the deposit and dissemination of scientific research documents, whether they are published or not. The documents may come from teaching and research institutions in France or abroad, or from public or private research centers.

L'archive ouverte pluridisciplinaire **HAL**, est destinée au dépôt et à la diffusion de documents scientifiques de niveau recherche, publiés ou non, émanant des établissements d'enseignement et de recherche français ou étrangers, des laboratoires publics ou privés.

A posteriori global error estimator based on the error in the constitutive relation for reduced basis approximation of parametrized linear elastic problems

L. Gallimard [a,*], D. Ryckelynck [b]

[a] *Laboratoire Energétique Mécanique Electromagnétisme EA4416, Université Paris Ouest Nanterre La Défense, 50 rue de Sèvres Ville d'Avray 92410, France*
[b] *MINES ParisTech, PSL, research university, Centre des Matériaux, CNRS UMR 7633, France*

Keywords:
Finite element analysis
Model reduction
Error bounds
Global error estimator
Reduced basis error indicator
Finite element error indicator

A B S T R A C T

In this paper we introduce a posteriori error estimator based on the concept of error in the constitutive relation to verify parametric models computed with a reduced basis approximation. We develop a global error estimator which leads to an upper bound for the exact error and takes into account all the error sources: the error due to the reduced basis approximation as well as the error due to the finite element approximation. We propose an error indicator to measure the quality of the reduced basis approximation and we deduce an error indicator on the finite element approximation.

1. Introduction

Finite Element Method is a common tool used to analyze and design parametrized mechanical systems. However, when a large set of parameters needs to be introduced in the model the computational effort increases drastically and many authors have recently shown interest in developing model reduction methods that exploit the fact that the response of complex models can often be approximated by the projection of the initial model on a low-dimensional reduced basis [1–4]. Reduced basis methods aim at speeding up the computational time for complex numerical models. They are based on an offline/online computational strategy which consist in determining in a first step a set of snapshots or a reduced basis (offline computations) that will be able to represent accurately the solutions for the problem studied. Different techniques are used to generate this basis, the more commonly found in the literature are the proper orthogonal decomposition and the greedy sampling approach [2,5]. In both case, the number of terms in the reduced basis is assumed to be very small compared to the number of degree of freedom of the finite element computation. Then, the approximate solutions of the parametrized problem are computed via performing a Galerkin projection onto the reduced basis space (online computations).

However, the accuracy of the obtained solutions depends on the quality of the mesh used as well as on the quality of the chosen reduced basis. If we denote by $\boldsymbol{\mu}$ the vector of parameters, the global error $\mathbf{e}_g$ is defined for any $\boldsymbol{\mu}$ by

$$\mathbf{e}_g(\boldsymbol{\mu}) = \mathbf{u}(\boldsymbol{\mu}) - \mathbf{u}_{rb}(\boldsymbol{\mu}), \tag{1}$$

* Corresponding author. Tel.: +33 140974865.
E-mail address: laurent.gallimard@u-paris10.fr (L. Gallimard).

where $\mathbf{u}(\boldsymbol{\mu})$ is the exact solution of the parametrized problem and $\mathbf{u}_{rb}(\boldsymbol{\mu})$ is its reduced basis approximation. This global error can be split into two parts:

$$\mathbf{e}_g(\boldsymbol{\mu}) = \mathbf{u}(\boldsymbol{\mu}) - \mathbf{u}_h(\boldsymbol{\mu}) + \mathbf{u}_h(\boldsymbol{\mu}) - \mathbf{u}_{rb}(\boldsymbol{\mu}) = \mathbf{e}_h(\boldsymbol{\mu}) + \mathbf{e}_{rb}(\boldsymbol{\mu}) \tag{2}$$

where $\mathbf{u}_h(\boldsymbol{\mu})$ is the finite element solution of the parametrized problem and $\mathbf{e}_{rb}(\boldsymbol{\mu}) = \mathbf{u}_h(\boldsymbol{\mu}) - \mathbf{u}_{rb}(\boldsymbol{\mu})$ (resp. $\mathbf{e}_h(\boldsymbol{\mu}) = \mathbf{u}(\boldsymbol{\mu}) - \mathbf{u}_h(\boldsymbol{\mu})$) is the error due to the projection of the finite element solution in the reduced basis space (resp. the error due to the finite element approximation). Within the framework and reduced basis approximations based on proper orthogonal decomposition or greedy sampling methods, many works have been devoted to the computation of a posteriori error estimators to measure the error due to the projection of the finite element solution in the reduced basis space. An error estimator is proposed for elliptic partial differential equations in [1,6], for parabolic problems in [7,8], for computational homogenization in [9], for stochastic computations [10]. However, the proposed error estimators are focused on the estimation of the error due to the reduced basis approximation $\mathbf{e}_{rb}$and assume that the error due to the finite element approximation $\mathbf{e}_h$ is negligible. Within the framework of the proper generalized decomposition, a global error estimator based on the concept of error in the constitutive relation [11], has been recently proposed for transient thermal problems in [12], and for linear elastic problems in [13]. This error estimator requires to develop a double reduced basis approximation during the offline step, a kinematic approach and a static approach, for solving the parametrized problem.

In this paper, we focus on parametrized linear elastic models where the parametric bilinear form a is depending on parameters-dependent functions in an affine manner. The objective of this paper is to extend the constitutive relation error estimator to reduced basis approximations based on greedy sampling. The use of the constitutive relation error (CRE) requires the computation of an admissible pair $(\hat{\mathbf{u}}, \hat{\boldsymbol{\sigma}})$ for any parameter $\boldsymbol{\mu}$ during the online computations. Unlike the approach proposed in [12,13], we use directly the initial reduced basis (i.e. the reduced basis used to compute the solution $\mathbf{u}_{rb}$) to build the admissible pair $(\hat{\mathbf{u}}, \hat{\boldsymbol{\sigma}})$ and we do not need to compute a second reduced basis by a greedy sampling algorithm. Additionally, two error indicators are developed to separate in the global error estimator the part of the error due to the finite element approximation from the part due to the reduced basis approximation. This family of error estimators allows to construct error bounds of the energy norm and has been applied to separate the contribution of the different sources of error in finite element computations for nonlinear problems [14–16], for domain decomposition problems [17,18]. We show that the global error estimator and the reduced basis error estimator are upper bounds of the corresponding exact errors. To compute efficiently the error estimates within the framework of an offline/online reduced basis method we need a further assumption, and we assume that the complementary energy is, as well as the bilinear form a, depending on parameters-dependent functions in an affine manner.

The paper is organized as follows: In Section 2, we introduce parametric problem to be solved, we briefly recall the reduced basis methodology, and we define the approximation errors introduced. The formulation of the global error estimator, the finite element error indicator and the reduced basis error indicator, as well as the offline/online strategy to compute them, are described in Section 3. Finally, in Section 4 the different errors are analyzed through a numerical example.

2. Problem to be solved

2.1. Linear elastic model

Let us consider an elastic structure defined in a domain Ω bounded by Γ. The external actions on the structure are represented by a surface force density $\mathbf{T}$ defined over a subset Γ_N of the boundary and a body force density $\mathbf{b}$ defined in Ω. We assume that a prescribed displacement $\mathbf{u} = \mathbf{u}_d$ is imposed on $\Gamma_D = \partial\Omega - \Gamma_N$. The material is assumed to be linear elastic, being $\mathbf{C}$the Hooke tensor. We consider that the problem is dependent of a set of parameters $\boldsymbol{\mu} \in \mathcal{D} \subset \mathbb{R}^p$. The problem can be formulated as: find a displacement field $\mathbf{u}(\boldsymbol{\mu}) \in \mathcal{U}$ and a stress field $\boldsymbol{\sigma}(\boldsymbol{\mu})$ defined in Ω which verify:

- the kinematic constraints:

$$\mathbf{u}(\boldsymbol{\mu}) = \mathbf{u}_d \text{ on } \Gamma_D \tag{3}$$

- the equilibrium equations:

$$\mathbf{div}\,\boldsymbol{\sigma}(\boldsymbol{\mu}) + \mathbf{b}(\boldsymbol{\mu}) = \mathbf{0} \text{ in } \Omega \text{ and } \boldsymbol{\sigma}(\boldsymbol{\mu})\mathbf{n} = \mathbf{T}(\boldsymbol{\mu}) \text{ in } \Gamma_N \tag{4}$$

- the constitutive equation:

$$\boldsymbol{\sigma}(\boldsymbol{\mu}) = \mathbf{C}(\boldsymbol{\mu})\boldsymbol{\varepsilon}(\mathbf{u}(\boldsymbol{\mu})) \text{ in } \Omega \tag{5}$$

$\mathbf{n}$ denotes the outgoing normal to Ω. $\mathcal{U}$ is the space in which the displacement field is being sought, $\mathcal{U}^0$ the space of the fields in $\mathcal{U}$ which are zero on Γ_D, and $\boldsymbol{\varepsilon}(\mathbf{u})$ denotes the linearized deformation associated with the displacement: $[\boldsymbol{\varepsilon}(\mathbf{u})]_{ij} = 1/2\,(u_{i,j} + u_{j,i})$.

The strong form of the problem (3-5) is equivalent to the classical weak form formulation: find $\mathbf{u} \in \{\mathbf{v} \in \mathcal{U};\ \mathbf{v}_{|\Gamma_D} = \mathbf{u}_d\}$ such that:

$$a(\mathbf{u}(\boldsymbol{\mu}), \mathbf{u}^*; \boldsymbol{\mu}) = f(\mathbf{u}^*; \boldsymbol{\mu}) \quad \forall \mathbf{u}^* \in \mathcal{U}^0 \tag{6}$$

where

$$a(\mathbf{u}(\boldsymbol{\mu}), \mathbf{u}^*; \boldsymbol{\mu}) = \int_\Omega \mathbf{C}(\boldsymbol{\mu})\boldsymbol{\varepsilon}(\mathbf{u}(\boldsymbol{\mu})) : \boldsymbol{\varepsilon}(\mathbf{u}^*)\, d\Omega \text{ and } f(\mathbf{u}^*; \boldsymbol{\mu}) = \int_\Omega \mathbf{b}(\boldsymbol{\mu}).\mathbf{u}^*\, d\Omega + \int_{\Gamma_N} \mathbf{T}(\boldsymbol{\mu}).\mathbf{u}^* d\Gamma$$

Following [1], we assume that the parametric bilinear form a and the loading f are affinely dependent of functions of the parameter $\boldsymbol{\mu}$, by which we shall mean:

$$a(\mathbf{u}, \mathbf{u}^*; \boldsymbol{\mu}) = \sum_{q=1}^{Q} \Theta^q(\boldsymbol{\mu}) a^q(\mathbf{u}, \mathbf{u}^*) \text{ and } f(\mathbf{u}^*; \boldsymbol{\mu}) = \sum_{q=1}^{Q'} H^q(\boldsymbol{\mu}) f^q(\mathbf{u}^*) \tag{7}$$

where $\Theta^q(\boldsymbol{\mu})(q \in \{1, \dots, Q\})$ and $H^q(\boldsymbol{\mu})(q \in \{1, \dots, Q'\})$ are known functions of $\boldsymbol{\mu}$, $a^q\,(q \in \{1, \dots, Q\})$ are bilinear forms independent of $\boldsymbol{\mu}$ and $f^q\,(q \in \{1, \dots, Q'\})$ are linear functions independent of $\boldsymbol{\mu}$.

Remark. This 'affine' decomposition has been successfully applied by Rozza et al. for different kind of parametrization: geometry, load intensity and direction, material properties, and multi subdomains for modular structures (see [2] for more details).

2.2. Finite element approximation

To compute the solution $\mathbf{u}(\boldsymbol{\mu})$ of Eq. (6), we introduce a finite element approximation $\mathbf{u}_h$ of $\mathbf{u}$ in a finite element space $\mathcal{U}_h$. The finite-dimension space $\mathcal{U}_h$ is associated with a finite element mesh of characteristic size h. Let $\mathcal{P}_h$ be a partition of Ω into elements E_k. This partition formed by the union of all elements, is assumed to coincide exactly with the domain Ω and any two elements are either disjoint or share a common edge. We assume that $\mathbf{u}_d$ can be represented by a displacement field in $\mathcal{U}_h$. The discretized problem is: find $\mathbf{u}_h \in \{\mathbf{v} \in \mathcal{U}_h;\ \mathbf{v}_{|\Gamma_D} = \mathbf{u}_d\}$ such that:

$$a(\mathbf{u}_h(\boldsymbol{\mu}), \mathbf{u}_h^*; \boldsymbol{\mu}) = f(\mathbf{u}_h^*; \boldsymbol{\mu}) \quad \forall \mathbf{u}_h^* \in \mathcal{U}_h^0 \tag{8}$$

where $\mathcal{U}_h^0 = \{\mathbf{v} \in \mathcal{U}_h; \mathbf{v}\,|_{\Gamma_D} = \mathbf{0}\}$.

The corresponding stress field is calculated using the constitutive equation:

$$\boldsymbol{\sigma}_h(\boldsymbol{\mu}) = \mathbf{C}(\boldsymbol{\mu})\boldsymbol{\varepsilon}(\mathbf{u}_h(\boldsymbol{\mu})) \tag{9}$$

2.3. Reduced basis approximation

Let $\mathbf{u}_{dir} \in \mathcal{U}_h$ be a displacement field such that $\mathbf{u}_{dir|\Gamma_D} = \mathbf{u}_d$. Let us introduce a set of samples in the parameter space $\mathcal{S}^{N_s} = \{\boldsymbol{\mu}^1, \dots, \boldsymbol{\mu}^{N_s}\}$, where $\boldsymbol{\mu}^i \in \mathcal{D}$, and for each $\boldsymbol{\mu}^n$ compute a finite element solution $\mathbf{u}_h^0(\boldsymbol{\mu}^n)$ in $\mathcal{U}_h^0$ described by the corresponding vector of nodal values $\mathbf{q}^n$.

$$a(\mathbf{u}_h^0(\boldsymbol{\mu}^n), \mathbf{u}_h^*; \boldsymbol{\mu}^n) = f(\mathbf{u}_h^*; \boldsymbol{\mu}^n) - a(\mathbf{u}_{dir}, \mathbf{u}_h^*; \boldsymbol{\mu}^n) \quad \forall \mathbf{u}_h^* \in \mathcal{U}_h^0 \tag{10}$$

The reduced basis space is then defined by

$$\mathcal{U}_{rb}^0 = \text{span}\{\mathbf{u}_h^0(\boldsymbol{\mu}^1), \dots, \mathbf{u}_h^0(\boldsymbol{\mu}^{N_s})\} \subset \mathcal{U}_h^0 \tag{11}$$

The choice of the samples in the parameter space $\mathcal{S}^{N_s}$ and of the associated reduced basis $\mathcal{U}_{rb}$ depends on the sampling strategy (see [1] for more details). In this paper, as detailed in Section 2.5, we use the Greedy approach proposed in [1,2]. The reduced basis approximation consists in solving Eq. (6) in $\mathcal{U}_{rb}^0 + \{\mathbf{u}_{dir}\}$. A key point to justify the use of the reduced basis approximation is that $N_s$is assumed to be much smaller than N_{fe} (i.e. $N_s \ll N_{fe}$).

$$a(\mathbf{u}_{rb}^0(\boldsymbol{\mu}), \mathbf{u}_{rb}^*; \boldsymbol{\mu}) = f(\mathbf{u}_{rb}^*; \boldsymbol{\mu}) - a(\mathbf{u}_{dir}, \mathbf{u}_{rb}^*; \boldsymbol{\mu}) \quad \forall \mathbf{u}_{rb}^* \in \mathcal{U}_{rb}^0 \tag{12}$$

Remark. The computation of $\mathbf{u}_{dir}$ is performed offline. The simplest choice is, for a given $\bar{\boldsymbol{\mu}} \in \mathcal{D}$, to find $\mathbf{u}_{dir} \in \{\mathbf{v} \in \mathcal{U}_h;\ \mathbf{v}_{|\Gamma_D} = \mathbf{u}_d\}$ such that

$$a(\mathbf{u}_{dir}, \mathbf{u}_h^*; \bar{\boldsymbol{\mu}}) = 0 \quad \forall \mathbf{u}_h^* \in \mathcal{U}_h^0$$

The corresponding stress field is calculated using the constitutive equation:

$$\boldsymbol{\sigma}_{dir} = \mathbf{C}(\bar{\boldsymbol{\mu}})\boldsymbol{\varepsilon}(\mathbf{u}_{dir}) \tag{13}$$

$\boldsymbol{\sigma}_{dir}$ is equilibrated to zero in the FE sense:

$$\int_\Omega \boldsymbol{\sigma}_{dir} : \boldsymbol{\varepsilon}(\mathbf{u}_h^*)\, d\Omega = 0, \quad \forall \mathbf{u}_h^* \in \mathcal{U}_h^0$$

Let us denote by Φ_{rb}^i the displacement fields $\mathbf{u}_h^0(\boldsymbol{\mu}^i)$ for $i \in \{1, \dots, N_s\}$. The reduced basis solution writes

$$\mathbf{u}_{rb}(\boldsymbol{\mu}) = \mathbf{u}_{dir} + \sum_{i=1}^{N_s} \alpha_i \Phi_{rb}^i \tag{14}$$

The corresponding stress is defined using the constitutive equation

$$\boldsymbol{\sigma}_{rb}(\boldsymbol{\mu}) = \mathbf{C}(\boldsymbol{\mu})\boldsymbol{\varepsilon}(\mathbf{u}_{dir}) + \sum_{i=1}^{N_s} \alpha_i \mathbf{C}(\boldsymbol{\mu})\boldsymbol{\varepsilon}(\Phi_{rb}^i) \tag{15}$$

by introducing Eq. (14) in Eq. (12) we build the algebraic system

$$[\mathbf{K}(\boldsymbol{\mu})][\boldsymbol{\alpha}] = [\mathbf{F}(\boldsymbol{\mu})] \tag{16}$$

The elements of $[\mathbf{K}(\boldsymbol{\mu})]$ and of $[\mathbf{F}(\boldsymbol{\mu})]$ are defined by

$$K_{ij}(\boldsymbol{\mu}) = a(\Phi_{rb}^i, \Phi_{rb}^j; \boldsymbol{\mu}) \text{ and } F_i(\boldsymbol{\mu}) = f(\Phi_{rb}^i; \boldsymbol{\mu}) \tag{17}$$

Thanks to the 'affine' decomposition of a and f, K_{ij} and F_i can be written as a linear combination of the functions $\Theta^q(\boldsymbol{\mu})(q \in \{1, \dots, Q\})$ and $H^q(\boldsymbol{\mu})(q \in \{1, \dots, Q'\})$.

$$K_{ij}(\boldsymbol{\mu}) = \sum_{q=1}^{Q} \Theta^q(\boldsymbol{\mu}) a^q(\Phi_{rb}^i, \Phi_{rb}^j) \text{ and } F_i(\boldsymbol{\mu}) = \sum_{q=1}^{Q'} H^q(\boldsymbol{\mu}) f^q(\Phi_{rb}^i) \tag{18}$$

A crucial point in reduced basis approximations is the separation of the computational procedure in two parts: an offline part devoted to the computation of parameters independent terms and performed only once, and an online part devoted to the computation of parameters dependent terms and performed many times. The computational complexity of the offline stage is great and depends on N_{fe} (the size of the finite element approximation), while the computational complexity of the online stage is small and depends on N_s , Q, Q'. We summarize the two parts of the computation (a more detailed description can be found in [1])

- offline: N_s finite element solutions $\Phi_{rb}^i = \mathbf{u}_h^0(\boldsymbol{\mu}^i)$ as well as the scalars quantities $a^q(\Phi_{rb}^i, \Phi_{rb}^j)$ and $f^q(\Phi_{rb}^i)$ are computed and stored.
- online: the matrix $[\mathbf{K}(\boldsymbol{\mu})]$ and the right hand side $[\mathbf{F}(\boldsymbol{\mu})]$ are assembled from Eq. (17), the system $[\mathbf{K}(\boldsymbol{\mu})][\boldsymbol{\alpha}] = [\mathbf{F}(\boldsymbol{\mu})]$ is solved and the displacement field $\mathbf{u}_{rb}(\boldsymbol{\mu})$ is computed from Eq. (14).

All the online operations are independent of dimension N_{fe} and depend only on N_s , Q and Q'.

2.4. Approximation errors

Two approximation errors are introduced in the computation of the reduced basis approximation

- an error due to the projection in the reduced basis space,
- an error due to the finite element approximation.

The global error $\mathbf{e}_g$ is defined by

$$\mathbf{e}_g(\boldsymbol{\mu}) = \mathbf{u}(\boldsymbol{\mu}) - \mathbf{u}_{rb}(\boldsymbol{\mu}) \tag{19}$$

This global error can be split in two parts

$$\mathbf{e}_g(\boldsymbol{\mu}) = \mathbf{e}_h(\boldsymbol{\mu}) + \mathbf{e}_{rb}(\boldsymbol{\mu}) \tag{20}$$

where $\mathbf{e}_h$ and $\mathbf{e}_{rb}$ are respectively the error introduced by the finite element approximation and the error introduced by the reduced basis approximation.

$$\mathbf{e}_h(\boldsymbol{\mu}) = \mathbf{u}(\boldsymbol{\mu}) - \mathbf{u}_h(\boldsymbol{\mu}) \text{ and } \mathbf{e}_{rb}(\boldsymbol{\mu}) = \mathbf{u}_h(\boldsymbol{\mu}) - \mathbf{u}_{rb}(\boldsymbol{\mu}) \tag{21}$$

The energy norm is a classical way to measure these errors

$$\|\mathbf{e}_\bullet(\boldsymbol{\mu})\|_{\boldsymbol{\mu}}^2 = a(\mathbf{e}_\bullet(\boldsymbol{\mu}), \mathbf{e}_\bullet(\boldsymbol{\mu}); \boldsymbol{\mu}) = \int_\Omega \mathbf{C}(\boldsymbol{\mu})\boldsymbol{\varepsilon}(\mathbf{e}_\bullet(\boldsymbol{\mu})) : \boldsymbol{\varepsilon}(\mathbf{e}_\bullet(\boldsymbol{\mu}))\, d\Omega \tag{22}$$

where $\bullet = g,\ h$ or rb. The following equality holds for the energy norm:

$$\|\mathbf{e}_g(\boldsymbol{\mu})\|_{\boldsymbol{\mu}}^2 = \|\mathbf{e}_h(\boldsymbol{\mu})\|_{\boldsymbol{\mu}}^2 + \|\mathbf{e}_{rb}(\boldsymbol{\mu})\|_{\boldsymbol{\mu}}^2 \tag{23}$$

2.5. Choice of the snapshots

The choice of the elements $\mathbf{u}_h(\boldsymbol{\mu}^i)$ of the reduced basis (often called snapshots) is performed following the Greedy approach proposed in [1,2]. We denote by $\mathcal{D}_{train} \subset \mathcal{D}$ the set of the samples which will be used to generate our reduced basis approximation and N_{train} the number of elements of $\mathcal{D}_{train}$. Typically $N_{train}$is chosen such that $N_s \ll N_{train}$. The generation of the snapshots is performed by an iterative greedy procedure. We begin with a first point $\boldsymbol{\mu}^1$ and a first reduced basis space $\mathcal{U}_{rb}^1 = \text{span}\{\mathbf{u}_h^0(\boldsymbol{\mu}^1)\}$, then, for $N = 2, \dots, N_s$, we compute $\mathbf{u}_{rb}(\boldsymbol{\mu})$ in $\mathcal{U}_{rb}^{N-1} + \{\mathbf{u}_{dir}\}$ for all $\boldsymbol{\mu} \in \mathcal{D}_{train}$ and we find

$$\boldsymbol{\mu}^N = \text{argmax}_{\boldsymbol{\mu} \in \mathcal{D}_{train}} \|\mathbf{e}_{rb}(\boldsymbol{\mu})\|_{\boldsymbol{\mu}} \text{ and } \mathbf{u}_h^0(\boldsymbol{\mu}^N) = \mathbf{u}_h(\boldsymbol{\mu}^N) - \mathbf{u}_{dir} \tag{24}$$

set $\mathcal{S}^N = \mathcal{S}^{N-1} \cup \boldsymbol{\mu}^N$, and update $\mathcal{U}_{rb}^N = \mathcal{U}_{rb}^{N-1} + \text{span}\{\mathbf{u}_h^0(\boldsymbol{\mu}^N)\}$.

Remark. For practical purpose it is necessary to replace $\|\mathbf{e}_{rb}(\boldsymbol{\mu})\|_{\boldsymbol{\mu}}$ by an inexpensive a posteriori error bound as proposed in [1]. In this paper, we use an error bound based on the concept of error in the constitutive relation that will be developed in Section (3.5).

3. Error in the constitutive relation

In this section, we propose an error estimation method based on the concept of error in the constitutive relation. We show that this error estimator is an upper bound of the error in the energy norm. An important point to develop an efficient error estimator for reduced basis approximations is that the cost of construction of the error estimators is independent on N_{fe}, and we need to introduce as a further assumption that the complementary energy is also affinely dependent of functions of the parameter $\boldsymbol{\mu}$.

$$\int_\Omega \mathbf{C}(\boldsymbol{\mu})^{-1}\boldsymbol{\sigma}_1 : \boldsymbol{\sigma}_2 \, d\Omega = \sum_{q=1}^{Q''} \Theta_\sigma^q(\boldsymbol{\mu}) \int_\Omega \mathbf{S}^q\boldsymbol{\sigma}_1 : \boldsymbol{\sigma}_2 \, d\Omega \tag{25}$$

where $\Theta_\sigma^q(\boldsymbol{\mu})$ are known scalar functions and $\mathbf{S}^q$ are fourth order tensor fields defined on Ω.

3.1. Definition of the error estimator

The approach based on the constitutive relation error [11] relies on a partition of the equations of the problem to be solved into two groups. In linear elasticity, the first group consists of the kinematic constraints and the equilibrium equations; the constitutive equation constitutes the second group. For a given $\boldsymbol{\mu} \in \mathcal{D}$, let us consider an approximate solution of the problem, denoted by $(\mathbf{u}^c, \boldsymbol{\sigma}^e)$, which verifies the first group of equations (3) and (4). This solution will be said *admissible*. If $(\mathbf{u}^c, \boldsymbol{\sigma}^e)$ verifies the constitutive equation (Eq. (5)) in Ω then $(\mathbf{u}^c, \boldsymbol{\sigma}^e) = (\mathbf{u}(\boldsymbol{\mu}), \boldsymbol{\sigma}(\boldsymbol{\mu}))$. If $(\mathbf{u}^c, \boldsymbol{\sigma}^e)$ does not verify the constitutive equation, the quality of this admissible solution is measured by the error in the constitutive relation $\eta_g$which is defined with respect to the constitutive equation

$$\eta_g = e_{cr}(\mathbf{u}^c, \boldsymbol{\sigma}^e) = \|\|\boldsymbol{\sigma}^e - \mathbf{C}(\boldsymbol{\mu})\boldsymbol{\varepsilon}(\mathbf{u}^c))\|\|_{\boldsymbol{\mu}} \tag{26}$$

where

$$\|\|\boldsymbol{\sigma}^e - \mathbf{C}(\boldsymbol{\mu})\boldsymbol{\varepsilon}(\mathbf{u}^c))\|\|_{\boldsymbol{\mu}} = \left[\int_\Omega (\boldsymbol{\sigma}^e - \mathbf{C}(\boldsymbol{\mu})\boldsymbol{\varepsilon}(\mathbf{u}^c)) : \mathbf{C}^{-1}(\boldsymbol{\mu})(\boldsymbol{\sigma}^e - \mathbf{C}(\boldsymbol{\mu})\boldsymbol{\varepsilon}(\mathbf{u}^c)) \, d\Omega\right]^{1/2} \tag{27}$$

The Prager–Synge theorem gives a relationship between the exact and admissible solution [19]

$$e_{cr}^2(\mathbf{u}^c, \boldsymbol{\sigma}^e) = \|\|\boldsymbol{\sigma} - \boldsymbol{\sigma}^e\|\|_{\boldsymbol{\mu}}^2 + \|\mathbf{u} - \mathbf{u}^c\|_{\boldsymbol{\mu}}^2 \tag{28}$$

3.2. Admissible solution

A key point to develop the error estimator is the construction, for a given $\boldsymbol{\mu} \in \mathcal{D}$, of an *admissible* solution $(\mathbf{u}^c, \boldsymbol{\sigma}^e)$ from the reduced basis solution $\mathbf{u}_{rb}(\boldsymbol{\mu})$ and the data. Since the reduced basis solution verifies the kinematic constraints, one takes:

$$\mathbf{u}^c = \mathbf{u}_{rb}(\boldsymbol{\mu}) \text{ in } \Omega \tag{29}$$

A method to recover equilibrated stress fields $\boldsymbol{\sigma}^e$ from the finite element solution and the data have been under development for several years [19–21]. In classical linear elasticity finite element computation, the admissible stress field can be constructed directly from the finite element stress field [19] because the finite element stress field verifies the equilibrium equations of the finite element model. In the case of a reduced basis the construction of an admissible stress field $\boldsymbol{\sigma}^e$ requires two distinct steps.

- In a first offline step, the reduced basis $\mathcal{U}_{rb}$ is used to build an admissible reduced basis for the stresses. This reduced basis is built with a recovery technique for constructing equilibrated stresses in star patches proposed in [20].
- In a second online step, the admissible stress is computed by a minimization of an energy norm.

3.3. Construction of an admissible stress field

The first step (offline) consists in building an admissible reduced basis for the stresses.

Let $\boldsymbol{\mu}^0$ denote a particular set of parameters such that $\boldsymbol{\mu}^0 \notin \{\boldsymbol{\mu}^1, \dots \boldsymbol{\mu}^{N_s}\}$, and let us introduce a set of displacement fields $\mathbf{u}_h^q(\boldsymbol{\mu}^0) \in \mathcal{U}_h^0$, for $q \in \{1, \dots, Q'\}$, such that

$$a(\mathbf{u}_h^q(\boldsymbol{\mu}^0), \mathbf{u}_h^*; \boldsymbol{\mu}^0) = f^q(\mathbf{u}_h^*) \quad \forall \mathbf{u}_h^* \in \mathcal{U}_h^0 \tag{30}$$

where f^q is the q^{th} element of the affine decomposition of the loading (Eq. (7)). The stress fields $\boldsymbol{\sigma}_f^q = \mathbf{C}(\boldsymbol{\mu}^0)\boldsymbol{\varepsilon}(\mathbf{u}_h^q(\boldsymbol{\mu}^0))$ verify an equilibrium equation in the FE sense (Eq. (31))

$$\int_\Omega \boldsymbol{\sigma}_f^q : \boldsymbol{\varepsilon}(\mathbf{u}_h^*) \, d\Omega = f^q(\mathbf{u}_h^*) \quad \forall \mathbf{u}_h^* \in \mathcal{U}_h^0 \tag{31}$$

For each $q \in \{1, \ldots, Q'\}$, a recovery technique [20] is used to build a stress field $\hat{\boldsymbol{\sigma}}_f^q$ that verifies the equilibrium equation defined by the following equation:

$$\int_\Omega \hat{\boldsymbol{\sigma}}_f^q : \boldsymbol{\varepsilon}(\mathbf{u}^*)\, d\Omega = f^q(\mathbf{u}^*) \quad \forall \mathbf{u}^* \in \mathcal{U}^0 \tag{32}$$

Similarly, a stress field $\hat{\boldsymbol{\sigma}}_{dir}$ equilibrated to zero is built from the stress field $\boldsymbol{\sigma}_{dir}$ (Eq. (13)) such that

$$\int_\Omega \hat{\boldsymbol{\sigma}}_{dir} : \boldsymbol{\varepsilon}(\mathbf{u}^*)\, d\Omega = 0 \quad \forall \mathbf{u}^* \in \mathcal{U}^0 \tag{33}$$

The set of stresses $\hat{\boldsymbol{\sigma}}_f^q$ is used to build an admissible stress field $\hat{\boldsymbol{\sigma}}_f(\boldsymbol{\mu})$ for any loading $f(\mathbf{u}^*; \boldsymbol{\mu})$. Let us define the stress field $\hat{\boldsymbol{\sigma}}_f(\boldsymbol{\mu})$, which depends explicitly on $\boldsymbol{\mu}$ by

$$\hat{\boldsymbol{\sigma}}_f(\boldsymbol{\mu}) = \sum_{q=1}^{Q'} H^q(\boldsymbol{\mu}) \hat{\boldsymbol{\sigma}}_f^q + \hat{\boldsymbol{\sigma}}_{dir} \tag{34}$$

where $H^q(\boldsymbol{\mu})$ are known functions of $\boldsymbol{\mu}$ defined in Eq. (7). If we introduce Eq. (32) in Eq. (7), thanks to the 'affine' decomposition, we obtain

$$\forall \mathbf{u}^* \in \mathcal{U}^0 \quad f(\mathbf{u}^*; \boldsymbol{\mu}) = \sum_{q=1}^{Q'} H^q(\boldsymbol{\mu}) \left(\int_\Omega \hat{\boldsymbol{\sigma}}_f^q : \boldsymbol{\varepsilon}(\mathbf{u}^*)\, d\Omega \right) = \int_\Omega \left(\sum_{q=1}^{Q'} H^q(\boldsymbol{\mu}) \hat{\boldsymbol{\sigma}}_f^q \right) : \boldsymbol{\varepsilon}(\mathbf{u}^*)\, d\Omega \tag{35}$$

Hence, the stress field $\hat{\boldsymbol{\sigma}}_f(\boldsymbol{\mu})$ is admissible for the loading $f(\mathbf{u}^*; \boldsymbol{\mu})$. Similarly $\boldsymbol{\sigma}_f(\boldsymbol{\mu})$ defined by Eq. (36) is an equilibrated stress field for the finite element model.

$$\boldsymbol{\sigma}_f(\boldsymbol{\mu}) = \sum_{q=1}^{Q'} H^q(\boldsymbol{\mu}) \boldsymbol{\sigma}_f^q + \boldsymbol{\sigma}_{dir} \tag{36}$$

The stress field $\hat{\boldsymbol{\sigma}}_f(\boldsymbol{\mu})$ could be used directly to compute an upper bound of the error, however it is easy to improve this upper bound adapting the technique proposed in [12] for a proper generalized decomposition method, to a reduced basis approach. Let us consider the set of stress fields computed from the snapshot solutions $\mathcal{U}_{rb}$

$$\boldsymbol{\sigma}_{rb}^i = \mathbf{C}(\boldsymbol{\mu}^i) \boldsymbol{\varepsilon}(\mathbf{u}_h(\boldsymbol{\mu}^i)) \text{ for } i \in \{1, \ldots, N_s\} \tag{37}$$

The stress field $\boldsymbol{\sigma}_{rb}^i$ is equilibrated in the FE sense for the loading $f(\mathbf{u}_h^*; \boldsymbol{\mu}^i)$. The recovery technique [20]is again used to compute admissible stress fields $\hat{\boldsymbol{\sigma}}_{rb}^i$ ($i \in \{1, \ldots, N_s\}$) such that

$$\int_\Omega \hat{\boldsymbol{\sigma}}_{rb}^i : \boldsymbol{\varepsilon}(\mathbf{u}^*)\, d\Omega = f(\mathbf{u}^*; \boldsymbol{\mu}^i) \quad \forall \mathbf{u}^* \in \mathcal{U}^0 \tag{38}$$

For a fixed $\boldsymbol{\mu}^i$ Eq. (34) leads to

$$\int_\Omega \hat{\boldsymbol{\sigma}}_f(\boldsymbol{\mu}^i) : \boldsymbol{\varepsilon}(\mathbf{u}^*)\, d\Omega = f(\mathbf{u}^*; \boldsymbol{\mu}^i) \quad \forall \mathbf{u}^* \in \mathcal{U}^0 \tag{39}$$

By subtracting Eq. (39) from Eq. (38) we obtain

$$\int_\Omega \Delta\hat{\boldsymbol{\sigma}}_{rb}^i : \boldsymbol{\varepsilon}(\mathbf{u}^*)\, d\Omega = 0 \quad \forall \mathbf{u}^* \in \mathcal{U}^0 \tag{40}$$

where $\Delta\hat{\boldsymbol{\sigma}}_{rb}^i = \hat{\boldsymbol{\sigma}}_{rb}^i - \hat{\boldsymbol{\sigma}}_f(\boldsymbol{\mu}^i) (i \in \{1, \ldots, N_s\})$ is a set of stress fields equilibrated to zero. Similarly,we can build a set of stress fields equilibrated to zero in the FE sense by setting $\Delta\boldsymbol{\sigma}_{rb}^i = \boldsymbol{\sigma}_{rb}^i - \boldsymbol{\sigma}_f(\boldsymbol{\mu}^i)$.

The second step of the construction is performed during the online procedure. For each parameter $\boldsymbol{\mu}$ an admissible stress field $\boldsymbol{\sigma}^e$ is sought in the reduced basis of equilibrated stress fields

$$\boldsymbol{\sigma}^e = \hat{\boldsymbol{\sigma}}_f(\boldsymbol{\mu}) + \sum_{i=1}^{N_s} \beta_i \Delta\hat{\boldsymbol{\sigma}}_{rb}^i \tag{41}$$

From Eqs. (40) and (34) it follows that $\boldsymbol{\sigma}^e$ is equilibrated with the loading $f(\mathbf{u}^*; \boldsymbol{\mu})$ for all $\beta_i \in \mathbb{R}$.

The coefficients β_i are computed in order to minimize the "distance" between the stress field computed in the reduced basis $\boldsymbol{\sigma}_{rb}(\boldsymbol{\mu}) = \mathbf{C}(\boldsymbol{\mu})\boldsymbol{\varepsilon}(\mathbf{u}_{rb})$ and a stress field equilibrated in the FE sense $\tilde{\boldsymbol{\sigma}}(\beta_1, \ldots, \beta_{N_s})$

$$J(\beta_1, \ldots, \beta_{N_s}) = \| |\mathbf{C}(\boldsymbol{\mu})\boldsymbol{\varepsilon}(\mathbf{u}_{rb}) - \tilde{\boldsymbol{\sigma}}(\beta_1, \ldots, \beta_{N_s})| \|_{\boldsymbol{\mu}} \tag{42}$$

where

$$\tilde{\boldsymbol{\sigma}}(\beta_1, \ldots, \beta_{N_s}) = \boldsymbol{\sigma}_f(\boldsymbol{\mu}) + \sum_{i=1}^{N_s} \beta_i \Delta\boldsymbol{\sigma}_{rb}^i \tag{43}$$

The minimization of Eq. (42) leads to the algebraic system

$$[\mathbf{A}(\boldsymbol{\mu})]\big[\boldsymbol{\beta}\big] = [\mathbf{G}(\boldsymbol{\mu})] \tag{44}$$

where

$$A_{ij} = \int_\Omega \mathbf{C}^{-1}(\boldsymbol{\mu})\Delta\boldsymbol{\sigma}^j_{rb} : \Delta\boldsymbol{\sigma}^i_{rb}\, d\Omega \tag{45}$$

and

$$G_j = \int_\Omega \Delta\boldsymbol{\sigma}^j_{rb} : (\boldsymbol{\varepsilon}(\mathbf{u}_{rb}) - \mathbf{C}^{-1}(\boldsymbol{\mu})\boldsymbol{\sigma}_f(\boldsymbol{\mu}))\, d\Omega \tag{46}$$

Remark. The equilibrated stress field $\boldsymbol{\sigma}^e$ could also be used in Eq. (42) instead of the weakly equilibrated stress field $\tilde{\boldsymbol{\sigma}}$, to obtain a better effectivity index for the global error estimator. However, the use of the weakly equilibrated stress field leads to minimize the error estimator on the reduced basis approximation (as shown in Eq. (61)) which is used to build the snapshots.

3.4. Computation of the error estimator and upper bound property

A direct application of the Prager–Synge theorem (Eq. (28)) with $\mathbf{u}^c = \mathbf{u}_{rb}$ and $\boldsymbol{\sigma}^e$ defined by Eq. (41) leads to the following upper bound property for the energy norm

$$\|\mathbf{e}_g(\boldsymbol{\mu})\|_{\boldsymbol{\mu}} = \|\mathbf{u} - \mathbf{u}_{rb}\|_{\boldsymbol{\mu}} \leq \eta_g = e_{cr}(\mathbf{u}_{rb}, \boldsymbol{\sigma}^e) \tag{47}$$

From Eq. (26) the expression of the global error estimator is given by

$$e^2_{cr}(\mathbf{u}_{rb}, \boldsymbol{\sigma}^e) = \int_\Omega \mathbf{C}^{-1}(\boldsymbol{\mu})\boldsymbol{\sigma}^e : \boldsymbol{\sigma}^e\, d\Omega + \int_\Omega \mathbf{C}(\boldsymbol{\mu})\boldsymbol{\varepsilon}(\mathbf{u}_{rb}) : \boldsymbol{\varepsilon}(\mathbf{u}_{rb})\, d\Omega - 2\int_\Omega \boldsymbol{\sigma}^e : \boldsymbol{\varepsilon}(\mathbf{u}_{rb})\, d\Omega \tag{48}$$

The computation of the global error estimator is done by an offline–online procedure

- During the offline procedure the stress fields $\hat{\boldsymbol{\sigma}}^q_f$ ($q \in \{1, \ldots, Q'\}$) and $\Delta\hat{\boldsymbol{\sigma}}^i_{rb}$($i \in \{1, \ldots, N_s\}$) are computed and stored, as well as the following scalar quantities for $(i, j) \in \{1, \ldots, N_s\}, p \in \{1, \ldots, Q'\}$ and $r \in \{1, \ldots, Q''\}$

$$\begin{aligned} a_{rij} &= \left(\int_\Omega \mathbf{S}^r \Delta\boldsymbol{\sigma}^i_{rb} : \Delta\boldsymbol{\sigma}^j_{rb}\, d\Omega\right) \\ a^0_{rpj} &= \left(\int_\Omega \mathbf{S}^r \boldsymbol{\sigma}^p_0 : \Delta\boldsymbol{\sigma}^j_{rb}\, d\Omega\right) \\ c_{ij} &= \left(\int_\Omega \Delta\boldsymbol{\sigma}^i_{rb} : \boldsymbol{\varepsilon}(\Phi^j_{rb}) d\Omega\right) \end{aligned} \tag{49}$$

and

$$\begin{aligned} \hat{a}_{rij} &= \int_\Omega \mathbf{S}^r \Delta\hat{\boldsymbol{\sigma}}^i_{rb} : \Delta\hat{\boldsymbol{\sigma}}^j_{rb}\, d\Omega \\ \hat{a}^0_{rpi} &= \int_\Omega \mathbf{S}^r \hat{\boldsymbol{\sigma}}^p_f : \Delta\hat{\boldsymbol{\sigma}}^i_{rb}\, d\Omega \\ \hat{a}^{00}_{rpq} &= \int_\Omega \mathbf{S}^r \hat{\boldsymbol{\sigma}}^p_f : \hat{\boldsymbol{\sigma}}^q_f\, d\Omega \\ \hat{b}_{sij} &= \int_\Omega \mathbf{C}^s \boldsymbol{\varepsilon}(\Phi^i_{rb}) : \boldsymbol{\varepsilon}(\Phi^j_{rb})\, d\Omega \\ \hat{c}_{ij} &= \int_\Omega \Delta\hat{\boldsymbol{\sigma}}^i_{rb} : \boldsymbol{\varepsilon}(\Phi^j_{rb})\, d\Omega \\ \hat{c}^0_{pi} &= \int_\Omega \hat{\boldsymbol{\sigma}}^p_f : \boldsymbol{\varepsilon}(\Phi^i_{rb})\, d\Omega \end{aligned} \tag{50}$$

- During the online procedure for each parameter $\boldsymbol{\mu}$, thanks to the 'affine' decomposition (Eq. (25)), we compute the coefficients of matrix $[\mathbf{A}(\boldsymbol{\mu})]$ and $[\mathbf{G}(\boldsymbol{\mu})]$ by introducing the coefficients defined by Eq. (49) in Eqs. (45) and (46):

$$A_{ij} = \sum_{r=1}^{Q''} \Theta^q_\sigma(\boldsymbol{\mu}) a_{rij} \text{ and } G_j = \sum_{i=1}^{N_s} \alpha_i(\boldsymbol{\mu}) c_{ij} - \sum_{p=1}^{Q'}\sum_{r=1}^{Q''} H^p(\boldsymbol{\mu})\Theta^r_\sigma(\boldsymbol{\mu}) a^0_{rpj} \tag{51}$$

then, the system $[\mathbf{A}(\boldsymbol{\mu})]\big[\boldsymbol{\beta}\big] = [\mathbf{G}(\boldsymbol{\mu})]$ is solved.

The error estimator e_{cr} is computed during the online procedure from the coefficients β_i, and the coefficients in Eq. (50) are computed during the offline procedure.

$$e^2_{cr}(\mathbf{u}_{rb}, \boldsymbol{\sigma}^e) = \sum_{r=1}^{Q''}\sum_{p=1}^{Q'}\sum_{q=1}^{Q'} \Theta^r_\sigma H^p H^q \hat{a}^{00}_{rpq} + \sum_{r=1}^{Q''}\sum_{p=1}^{Q'}\sum_{i=1}^{N_s} \Theta^r_\sigma H^p \beta_i \hat{a}^0_{rpi}$$

$$+\sum_{r=1}^{Q''}\sum_{i=1}^{N_s}\sum_{j=1}^{N_s}\Theta_\sigma^r\beta_i\beta_j\hat{a}_{rij}+\sum_{s=1}^{Q}\sum_{i=1}^{N_s}\sum_{j=1}^{N_s}\Theta^s\alpha_i\alpha_j\hat{b}_{sij}$$
$$-2\sum_{p=1}^{Q'}\sum_{i=1}^{N_s}H^p\alpha_i\hat{c}^0_{pi}-2\sum_{i=1}^{N_s}\sum_{j=1}^{N_s}\beta_i\alpha_j\hat{c}_{ij} \tag{52}$$

All the online computations are independent on N_{fe} and depend only on Q, Q', Q'', and N_s

3.5. Error indicators

The error estimator in the constitutive relation $e_{cr}(\mathbf{u}^c, \boldsymbol{\sigma}^e)$ defined in Section 3.4 is a global error estimator which takes into account the errors due to the projection in the reduced basis space as well as the error due to the finite element approximation. In order to control the global error, it is important to separate in this global error the different error contributions and to build error indicators which can measure separately the error contributions from the reduced basis approximation and the error contributions from the finite element approximation. A first approach to build error indicators based on the error in the constitutive relation was proposed for separating time integration error from finite element spatial error in elasto-plasticity [14,16,22,23], the same idea was applied to domain decomposition algorithms in [17,18]. Within the framework of the proper generalized decomposition separated error indicators were proposed in [12].

To estimate the contribution to the global error due to the reduced basis approximation, we define a new reference model that is the finite element model: Find a displacement field $\mathbf{u}_h(\boldsymbol{\mu}) \in \mathcal{U}_h$ and a stress field $\boldsymbol{\sigma}_h(\boldsymbol{\mu})$ defined in Ω which verify:

- the kinematic constraints:

$$\mathbf{u}_h(\boldsymbol{\mu}) = \mathbf{u}_d \text{ on } \Gamma_D \tag{53}$$

- the finite element equilibrium equations:

$$\int_\Omega \boldsymbol{\sigma}_h(\boldsymbol{\mu}) : \boldsymbol{\varepsilon}(\mathbf{u}_h^*)\, d\Omega = \int_\Omega \mathbf{b}(\boldsymbol{\mu}).\mathbf{u}_h^*\, d\Omega + \int_{\Gamma_N} \mathbf{T}(\boldsymbol{\mu}).\mathbf{u}_h^* d\Gamma \quad \forall \mathbf{u}_h^* \in \mathcal{U}_h^0 \tag{54}$$

- the constitutive equation:

$$\boldsymbol{\sigma}_h(\boldsymbol{\mu}) = \mathbf{C}(\boldsymbol{\mu})\boldsymbol{\varepsilon}(\mathbf{u}_h(\boldsymbol{\mu})) \text{ in } \Omega \tag{55}$$

Let us consider an approximate solution of the problem, denoted by $(\mathbf{u}^{cef}, \boldsymbol{\sigma}^{eef})$ which verifies the first group of equations (Eqs. (53) and (54)). This solution will be said to be *FE-admissible*. If $(\mathbf{u}^{cef}, \boldsymbol{\sigma}^{eef})$ verifies the constitutive equation (Eq. 55) in Ω then $(\mathbf{u}^{cef}, \boldsymbol{\sigma}^{eef}) = (\mathbf{u}_h(\boldsymbol{\mu}), \boldsymbol{\sigma}_h(\boldsymbol{\mu}))$. If $(\mathbf{u}^{cef}, \boldsymbol{\sigma}^{eef})$ does not verify the constitutive equation, the quality of this admissible solution is measured by the error in the constitutive relation η_{rb}which is defined with respect to the constitutive equation

$$\eta_{rb} = e_{cr}(\mathbf{u}^{cef}, \boldsymbol{\sigma}^{eef}) = \|\,|\boldsymbol{\sigma}^{eef} - \mathbf{C}(\boldsymbol{\mu})\boldsymbol{\varepsilon}(\mathbf{u}^{cef}))\|\,|_{\boldsymbol{\mu}} \tag{56}$$

The *FE-admissible* fields can be constructed straightforwardly from the previous computations. Since the reduced basis solution $\mathbf{u}_{rb}(\boldsymbol{\mu})$ verifies the kinematic constraints and since the stress field $\tilde{\boldsymbol{\sigma}}(\beta_1, \ldots, \beta_{N_s})$ computed by Eq. (43) is equilibrated in the FE sense (i.e. verifies Eq. (54)), one takes $(\mathbf{u}^{cef}, \boldsymbol{\sigma}^{eef}) = (\mathbf{u}_{rb}(\boldsymbol{\mu}), \tilde{\boldsymbol{\sigma}}(\beta_1, \ldots, \beta_{N_s}))$.

The application of the Prager–Synge theorem to $\eta_{rb} = e_{cr}(\mathbf{u}_{rb}(\boldsymbol{\mu}), \tilde{\boldsymbol{\sigma}})$ shows that η_{rb} is an upper bound of the error for the reduced basis approximation. Let us consider

$$\eta_{rb}^2 = |\,\|\tilde{\boldsymbol{\sigma}} - \mathbf{C}\boldsymbol{\varepsilon}(\mathbf{u}_{rb}))\|\,|_{\boldsymbol{\mu}}^2 \tag{57}$$

As $\boldsymbol{\sigma}_h - \mathbf{C}\boldsymbol{\varepsilon}(\mathbf{u}_h) = 0$, we have

$$\eta_{rb}^2 = |\,\|\tilde{\boldsymbol{\sigma}} - \boldsymbol{\sigma}_h + \mathbf{C}\boldsymbol{\varepsilon}(\mathbf{u}_h) - \mathbf{C}\boldsymbol{\varepsilon}(\mathbf{u}_{rb})\|\,|_{\boldsymbol{\mu}}^2 \tag{58}$$

This expression can be developed in

$$\eta_{rb}^2 = |\,\|\tilde{\boldsymbol{\sigma}} - \boldsymbol{\sigma}_h\|\,|_{\boldsymbol{\mu}}^2 + \|\mathbf{u}_h - \mathbf{u}_{rb}\|_{\boldsymbol{\mu}}^2 + 2\int_\Omega (\tilde{\boldsymbol{\sigma}} - \boldsymbol{\sigma}_h) : \boldsymbol{\varepsilon}(\mathbf{u}_h - \mathbf{u}_{rb}) d\Omega \tag{59}$$

As $\boldsymbol{\sigma}_h$ and $\tilde{\boldsymbol{\sigma}}$ verify Eq. (54) and $\mathbf{u}_h - \mathbf{u}_{rb} \in \mathcal{U}_h^0$, we have

$$\int_\Omega (\tilde{\boldsymbol{\sigma}} - \boldsymbol{\sigma}_h) : \boldsymbol{\varepsilon}(\mathbf{u}_h - \mathbf{u}_{rb}) d\Omega = 0 \tag{60}$$

and

$$\eta_{rb}^2 = e_{cr}^2(\mathbf{u}_{rb}, \tilde{\boldsymbol{\sigma}}) = \|\,|\boldsymbol{\sigma}_h - \tilde{\boldsymbol{\sigma}}\|\,|_{\boldsymbol{\mu}}^2 + \|\mathbf{u}_h - \mathbf{u}_{rb}\|_{\boldsymbol{\mu}}^2 \tag{61}$$

As a consequence η_{rb} is an upper bound of the error for the reduced basis approximation

$$\|\mathbf{e}_{rb}(\boldsymbol{\mu})\|_{\boldsymbol{\mu}} = \|\mathbf{u}_h - \mathbf{u}_{rb}\|_{\boldsymbol{\mu}} \leq \eta_{rb} \tag{62}$$

It will be shown in the numerical examples that the computed upper bound is very sharp. This error indicator is used to replace $\|\mathbf{e}_{rb}(\boldsymbol{\mu})\|_{\boldsymbol{\mu}}$ in Eq. (24) for the choice of the snapshots.

The error indicator on the reduced basis error η_{rb} is computed by an online/offline procedure similar to the procedure used in Section 3.4 to compute the global error estimator.

To estimate the part of the error due to the finite element discretization $\|\mathbf{e}_h\|_{\boldsymbol{\mu}}$, we introduce an error indicator η_{fe} which can be directly deduced from η_g and η_{rb}. This error indicator is not an upper bound of $\|\mathbf{e}_h\|_{\boldsymbol{\mu}}$, however it provides a pertinent estimate of the discretization error. This error indicator is based on the following equality:

$$\eta_g^2 = \eta_{rb}^2 + \|\|\boldsymbol{\sigma}_h - \boldsymbol{\sigma}^e\|\|_{\boldsymbol{\mu}}^2 - \|\|\boldsymbol{\sigma}_h - \tilde{\boldsymbol{\sigma}}\|\|_{\boldsymbol{\mu}}^2 \tag{63}$$

This result is deduced from the properties of the $FE-admissible$ stress field $\tilde{\boldsymbol{\sigma}}$ and the *admissible* stress field $\boldsymbol{\sigma}^e$. As $\mathbf{u}_h - \mathbf{u}_{rb} \in \mathcal{U}_h^0$ we have the following Galerkin orthogonality relation

$$\int_\Omega (\boldsymbol{\sigma}^e - \tilde{\boldsymbol{\sigma}}) : \boldsymbol{\varepsilon}(\mathbf{u}_h - \mathbf{u}_{rb})\, d\Omega = 0 \tag{64}$$

and

$$\begin{aligned}\|\|\boldsymbol{\sigma}^e - \boldsymbol{\sigma}_h\|\|_{\boldsymbol{\mu}}^2 &= \|\|\boldsymbol{\sigma}^e - \tilde{\boldsymbol{\sigma}}\|\|_{\boldsymbol{\mu}}^2 + \|\|\tilde{\boldsymbol{\sigma}} - \boldsymbol{\sigma}_h\|\|_{\boldsymbol{\mu}}^2 \\ &\quad + 2\int_\Omega (\boldsymbol{\sigma}^e - \tilde{\boldsymbol{\sigma}}) : C^{-1}(\boldsymbol{\mu})(\tilde{\boldsymbol{\sigma}} - \boldsymbol{\sigma}_h)\, d\Omega\end{aligned} \tag{65}$$

From Eqs. (65) and (64) we can deduce that

$$\begin{aligned}2\int_\Omega (\boldsymbol{\sigma}^e - \tilde{\boldsymbol{\sigma}}) : C^{-1}(\boldsymbol{\mu})(\tilde{\boldsymbol{\sigma}} - \boldsymbol{\sigma}_{rb})\, d\Omega &= \|\|\boldsymbol{\sigma}^e - \boldsymbol{\sigma}_h\|\|_{\boldsymbol{\mu}}^2 \\ &\quad - \|\|\boldsymbol{\sigma}^e - \tilde{\boldsymbol{\sigma}}\|\|_{\boldsymbol{\mu}}^2 - \|\|\tilde{\boldsymbol{\sigma}} - \boldsymbol{\sigma}_h\|\|_{\boldsymbol{\mu}}^2\end{aligned} \tag{66}$$

Moreover

$$\begin{aligned}\eta_g^2 &= \|\|\boldsymbol{\sigma}^e - \tilde{\boldsymbol{\sigma}}\|\|_{\boldsymbol{\mu}}^2 + \|\|\tilde{\boldsymbol{\sigma}} - \boldsymbol{\sigma}_{rb}\|\|_{\boldsymbol{\mu}}^2 \\ &\quad + 2\int_\Omega (\boldsymbol{\sigma}^e - \tilde{\boldsymbol{\sigma}}) : C^{-1}(\boldsymbol{\mu})(\tilde{\boldsymbol{\sigma}} - \boldsymbol{\sigma}_{rb})\, d\Omega\end{aligned} \tag{67}$$

By introducing Eq. (66) in Eq. (67) we obtain

$$\eta_g^2 = \|\|\tilde{\boldsymbol{\sigma}} - \boldsymbol{\sigma}_{rb}\|\|_{\boldsymbol{\mu}}^2 + \|\|\boldsymbol{\sigma}_h - \boldsymbol{\sigma}^e\|\|_{\boldsymbol{\mu}}^2 - \|\|\boldsymbol{\sigma}_h - \tilde{\boldsymbol{\sigma}}\|\|_{\boldsymbol{\mu}}^2 \tag{68}$$

which concludes the proof.

Under the assumption that $\|\|\boldsymbol{\sigma}_h - \tilde{\boldsymbol{\sigma}}\|\|_{\boldsymbol{\mu}} < \|\|\boldsymbol{\sigma}_h - \boldsymbol{\sigma}^e\|\|_{\boldsymbol{\mu}}$, we can estimate the contribution to the global error due to the finite element approximation by defining the following error indicator η_{fe}

$$\eta_{fe} = \sqrt{\eta_g^2 - \eta_{rb}^2} \tag{69}$$

As far we know we cannot prove that $\|\|\boldsymbol{\sigma}_h - \tilde{\boldsymbol{\sigma}}\|\|_{\boldsymbol{\mu}} < \|\|\boldsymbol{\sigma}_h - \boldsymbol{\sigma}^e\|\|_{\boldsymbol{\mu}}$, however in practical computation we can observe that $\eta_{rb} < \eta_g$. The relation between η_{fe} and $\|\mathbf{e}_h\|_{\boldsymbol{\mu}}$ is given by

$$\eta_{fe}^2 = \|\mathbf{e}_h\|_{\boldsymbol{\mu}}^2 + \|\|\boldsymbol{\sigma} - \boldsymbol{\sigma}^e\|\|_{\boldsymbol{\mu}}^2 - \|\|\boldsymbol{\sigma}_h - \boldsymbol{\sigma}^{eef}\|\|_{\boldsymbol{\mu}}^2 \tag{70}$$

$\boldsymbol{\sigma}$ being the "exact" stress defined by Eqs. (3-5). This equality is easily obtained by using the Prager–Synge theorem on $(\mathbf{u}_h, \boldsymbol{\sigma}^e)$

$$\|\|\boldsymbol{\sigma}^e - \boldsymbol{\sigma}_h\|\|_{\boldsymbol{\mu}}^2 = \|\|\boldsymbol{\sigma} - \boldsymbol{\sigma}^e\|\|_{\boldsymbol{\mu}}^2 + \|\|\boldsymbol{\sigma} - \boldsymbol{\sigma}_h\|\|_{\boldsymbol{\mu}}^2 = \|\|\boldsymbol{\sigma} - \boldsymbol{\sigma}^e\|\|_{\boldsymbol{\mu}}^2 + \|\mathbf{e}_h\|_{\boldsymbol{\mu}}^2 \tag{71}$$

and introducing Eq. (71) in Eq. (63).

Eq. (70) shows that η_{fe} is not an upper bound of $\|\mathbf{e}_h\|_{\boldsymbol{\mu}}$. However, it can be used as an error indicator for the part of the error due to the FE computation when the mesh is not too coarse, as it will be shown in the numerical examples.

4. Numerical results

This section is devoted to the numerical study of the error estimates and bounds presented in previous sections. We consider the case where the structure Ω is composed of N different subdomains Ω^i, and where each subdomain is made of a homogeneous elastic material. The components of the vector of parameters $\boldsymbol{\mu}$ are the coefficients of the elastic tensors $\mathbf{C}^i$.

$$\Omega = \bigcup_{i=1}^{N} \Omega^i$$

The bilinear form a is decomposed in

$$a(\mathbf{u}, \mathbf{v}; \boldsymbol{\mu}) = \sum_{i=1}^{N} \mathbf{C}^i(\boldsymbol{\mu}) \int_{\Omega^i} \boldsymbol{\varepsilon}(\mathbf{u}) : \boldsymbol{\varepsilon}(\mathbf{v})\, dV$$

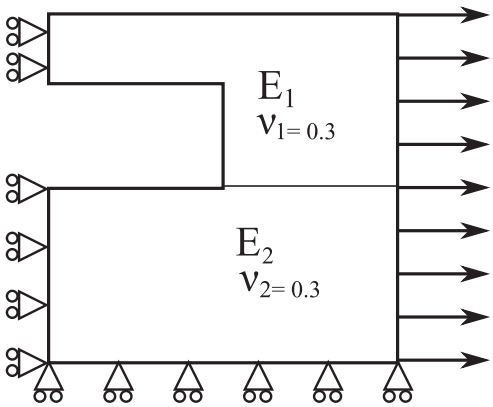

Fig. 1. Thin plate studied.

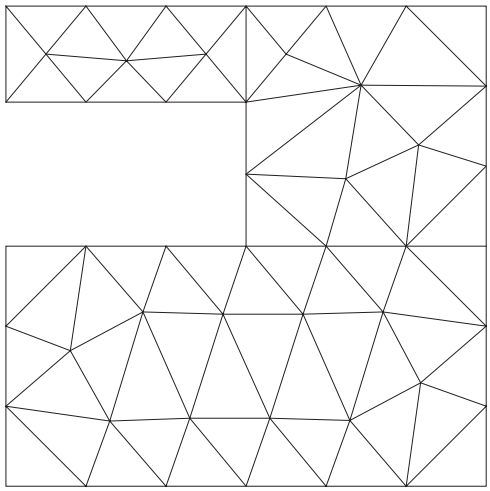

Fig. 2. Mesh M3: 326 DoF .

The complementary energy is decomposed in

$$\int_{\Omega} \mathbf{C}^{-1}(\boldsymbol{\mu})\boldsymbol{\sigma}_1 : \boldsymbol{\sigma}_2 dV = \sum_{i=1}^{N} \left(\mathbf{C}^i(\boldsymbol{\mu})\right)^{-1} \int_{\Omega^i} \boldsymbol{\sigma}_1 : \boldsymbol{\sigma}_2 \, dV.$$

4.1. Description of the studied problem

The studied structure is a thin plate with two rectangular holes proposed in [24]. Normal traction is applied along the vertical edge and the plate is considered to be composed of two different materials. The symmetry of the problem allows to study only one fourth of the plate as shown on Fig. (1). The Young modulus E_1 is fixed to 200 *GPa* and E_2 varies from 0.1 E_1 to 10 E_1. The Poisson ratios are fixed $\nu_1 = \nu_2 = 0.30$. The problem depends on one parameter $\boldsymbol{\mu} = (\mu) \in \mathcal{D} \subset \mathbb{R}$, with $\mathcal{D} = [0.1, 10]$. We choose the set $\mathcal{D}_{train} \subset \mathcal{D}$ such that $\mathcal{D}_{train} = \{\mu_i = c_{min}(c_{max}/c_{min})^{(i/n_{train})};\ i = 0, \ldots, N_{train}\}$, with $c_{min} = 0.1, c_{max} = 10$, and $N_{train} = 100$. The first point in the parameter set used to build the reduced basis is $\mu^1 = 1$.

4.2. Computation of the error estimators

In this section the reduced basis solution is computed for different values of the parameters $\mu = 0.2, 0.5, 2., 8.0 \in \mathcal{D}$, and we present the evolution of the error estimators as the mesh and the size of the reduced basis vary. 6-nodes triangular elements are used to mesh the structure. We first study the evolution of the error estimators η_g, η_{rb} and η_h for a fixed mesh (Fig. 2) when the number of snapshots N_s increases. The generation of the snapshots is performed by the iterative greedy procedure described in Section 2.5 for $N_s = 6$. The successive values of the μ parameter are: {1.00, 0.10, 10.0, 0.23, 3.98, 0.46}.

The computed error estimators are given in Fig. (3). It is interesting to note that the reduced basis error indicator converges rapidly toward zero. We see also that η_h provides a good assessment of the finite element error even when N_s is small. The global

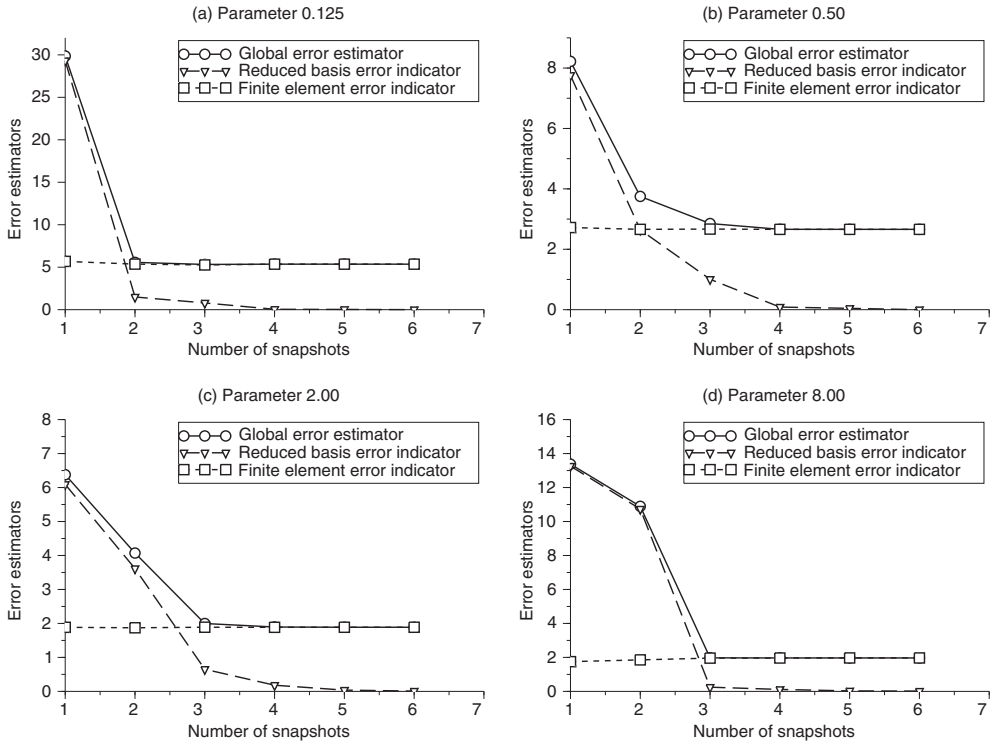

Fig. 3. Evolution of the error estimators η_g, η_{rb}, η_h as a function of the number of snapshots for (a) $\mu = 0.125$, (b) $\mu = 0.50$, (c) $\mu = 2.0$, (d) $\mu = 8.0$.

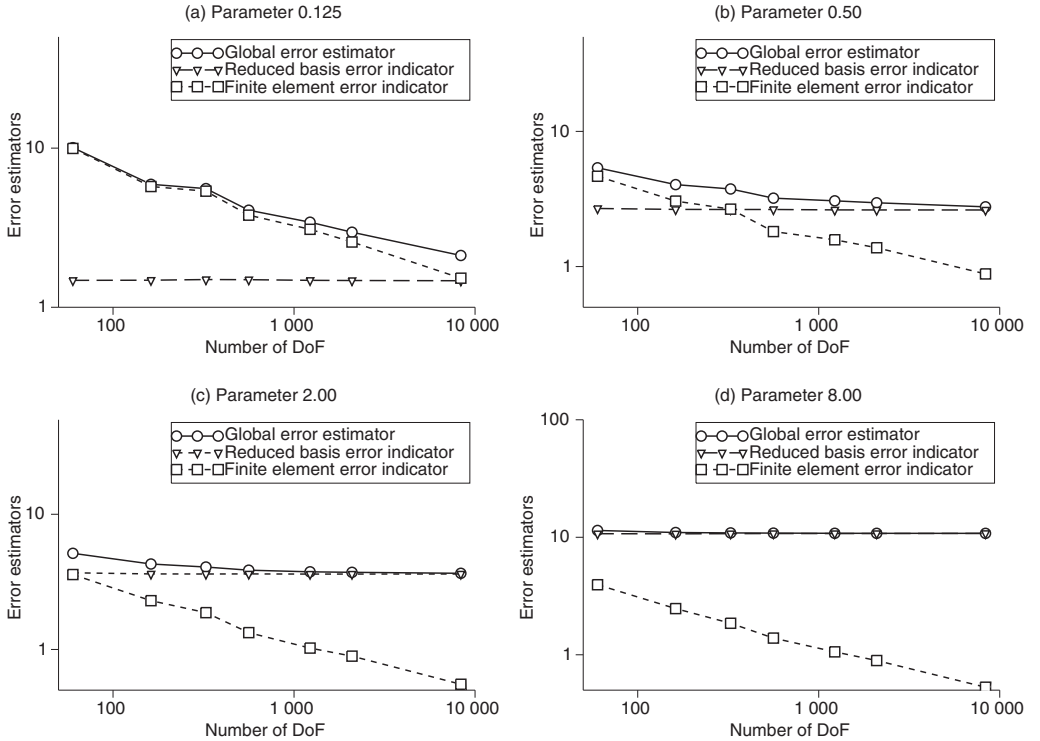

Fig. 4. Evolution of the error estimators η_g, η_{rb}, η_h as a function of the number DoF for $N_s = 2$ and (a) $\mu = 0.125$, (b) $\mu = 0.50$, (c) $\mu = 2.0$, (d) $\mu = 8.0$.

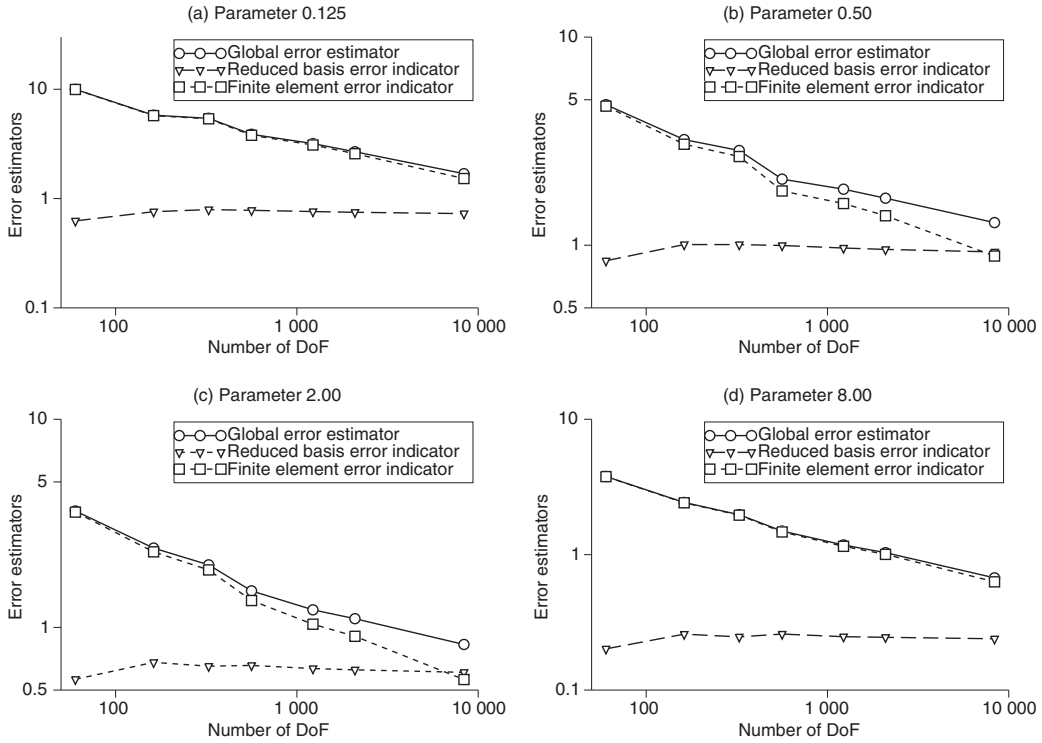

Fig. 5. Evolution of the error estimators η_g, η_{rb}, η_h as a function of the number DoF for $N_s = 3$ and (a) $\mu = 0.125$, (b) $\mu = 0.50$, (c) $\mu = 2.0$, (d) $\mu = 8.0$.

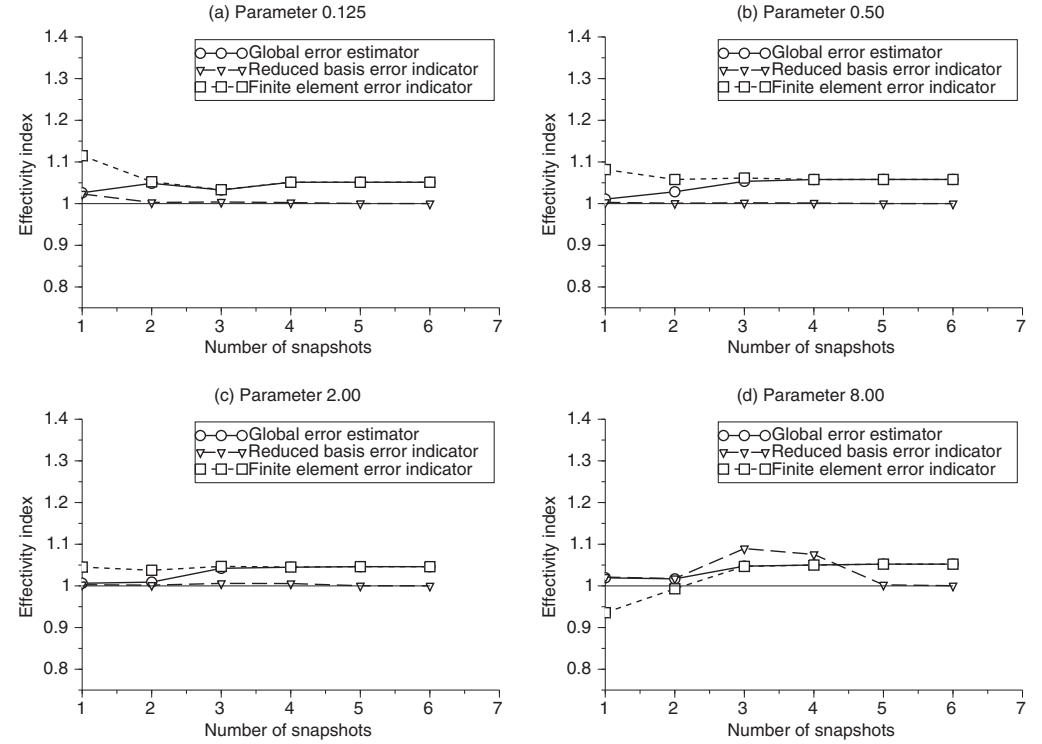

Fig. 6. Evolution of the effectivity indexes θ_g, θ_{rb}, θ_h as a function of the number of snapshots for (a) $\mu = 0.125$, (b) $\mu = 0.50$, (c) $\mu = 2.0$, (d) $\mu = 8.0$.

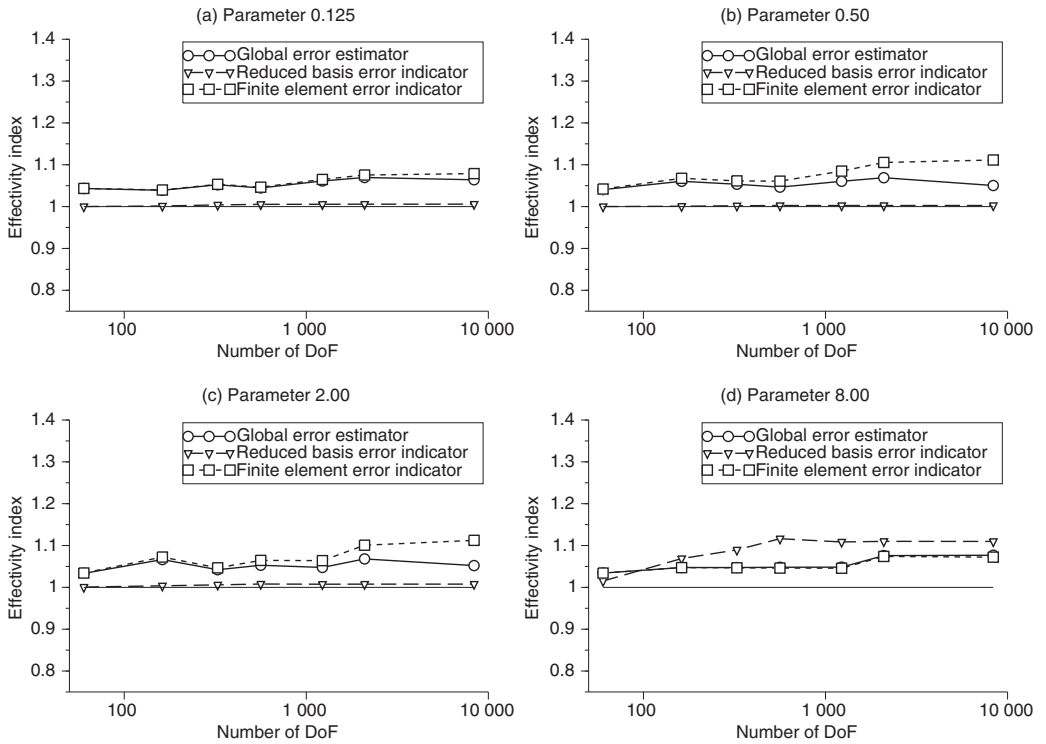

Fig. 7. Evolution of the effectivity indexes θ_g, θ_{rb}, θ_h as a function of the number DoF for $N_s = 3$ and (a) $\mu = 0.125$, (b) $\mu = 0.50$, (c) $\mu = 2.0$, (d) $\mu = 8.0$.

error tends to a horizontal asymptote which is the finite element discretization error, and it can be seen that increasing the number of snapshots above 4 does not improve the quality of the solution. Fig. (4) shows the evolution of the error estimators for uniformly-refined meshes when the number of snapshots is fixed to $N_s = 2$. The reduced basis error indicator η_{rb}, is very little sensitive to the mesh. For parameter $\mu = 0.125$ it can be seen that the reduced basis indicator is very small. For parameters $\mu = 0.50, 2.00$ and 8.00 the reduced basis error indicator is greater and the global error estimator tends rapidly to a horizontal asymptote which means that it is not necessary to refine the mesh if the reduced basis is not improved. Nevertheless the finite element error indicator η_h decreases with the number of degree of freedom (DoF). Fig. (5) shows the evolution of the error estimators for uniformly-refined meshes when the number of snapshots if fixed to $N_s = 3$. The reduced basis error indicator η_{rb} is very small, and the mesh refinement increases the quality of the computation.

4.3. Computation of the effectivity indexes

The quality of the error estimators is measured with the effectivity index

$$\theta = \frac{\text{estimated error norm}}{\text{“true” error norm}} \tag{72}$$

where the “true” error norm is either the exact error if available, or a reference error computed from a refined mesh if the true error is unavailable. In this paper we consider three different effectivity indexes computed from the error fields defined in Eqs. (19-21).

$$\theta_g = \frac{\eta_g}{\|\mathbf{e}_g\|_\mu},\ \theta_{rb} = \frac{\eta_{rb}}{\|\mathbf{e}_{rb}\|_\mu} \text{ and } \theta_h = \frac{\eta_h}{\|\mathbf{e}_h\|_\mu} \tag{73}$$

Three displacement fields are necessary to compute these errors for a given $\boldsymbol{\mu}$: $\mathbf{u}(\boldsymbol{\mu})$, $\mathbf{u}_h(\boldsymbol{\mu})$, $\mathbf{u}_{rb}(\boldsymbol{\mu})$. $\mathbf{u}_{rb}(\boldsymbol{\mu})$ is obtained directly from the reduced basis computation, $\mathbf{u}_h(\boldsymbol{\mu})$ is computed exactly by performing a finite element computation, and an approximation $\mathbf{u}_{ref}(\boldsymbol{\mu})$ of $\mathbf{u}(\boldsymbol{\mu})$ is computed on a refined mesh. We get

$$\|\mathbf{e}_g\|_\mu \approx \|\mathbf{u}_{ref}(\boldsymbol{\mu}) - \mathbf{u}_{rb}(\boldsymbol{\mu})|_\mu,\ \|\mathbf{e}_{rb}\|_\mu = \|\mathbf{u}_h(\boldsymbol{\mu}) - \mathbf{u}_{rb}(\boldsymbol{\mu})\|_\mu \text{ and } \|\mathbf{e}_h\|_\mu \approx \|\mathbf{u}_{ref}(\boldsymbol{\mu}) - \mathbf{u}_h(\boldsymbol{\mu})\|_\mu \tag{74}$$

Fig. (6) shows the evolution of the effectivity indexes for a fixed mesh (Fig. 2) when the number of snapshots N_s increases. θ_g and θ_{rb} are greater than 1, which illustrates the upper bound property for the global error estimator η_g and the reduced basis error indicator η_{rb}. Moreover the computed bounds are, on this example, rather sharp with values in [1., 1.2]. (Fig. 6(d)) illustrates that η_h is not necessarily an upper bound of the finite element error ($\theta_h < 1$ when the number of snapshots is lesser that 2), nevertheless θ_h becomes greater than 1 when the number of snapshots increases. Fig. (7) shows the evolution of the effectivity indexes for a fixed number of snapshots when the number of Dof increases.

5. Conclusions

This paper introduces an error estimator based on the constitutive relation which provides an upper bound of the global error for parametric linear elastic models computed with a reduced basis approximation. This error estimator takes into account all the errors due to the approximations introduced (i.e. both the finite element and the reduced basis approximations). Two error indicators are developed to estimate the contributions of each source of error. The reduced basis error indicator is defined in the same way as the global error, except that the reference problem is different, and provides an upper bound for the reduced basis error. The finite element error indicator is defined by using the orthogonality property between the finite element error and the reduced basis error. With these tools, the next step, which is under consideration is to use these error estimators to compute bounds for outputs of interest. The extension of this error estimator to parametrized geometries (see [1]) would allow to consider a larger class of problems of interest.

References

[1] G. Rozza, D.B.P. Huynh, A.T. Patera, Reduced basis approximation and a posteriori error estimation for affinely parametrized elliptic coercive partial differential equations, Arch. Comput. Methods Eng. 15 (2008) 229–275.
[2] R. Milani, A. Quarteroni, G. Rozza, Reduced basis method for linear elasticity problems with many parameters, Comput. Methods Appl. Mech. Eng. 197 (51-52) (2008) 4812–4829. http://dx.doi.org/10.1016/j.cma.2008.07.002.
[3] S. Boyaval, C. Le Bris, Y. Maday, N.C. Nguyen, A.T. Patera, Reduced basis approach for variational problems with stochastic parameters: application to heat conduction with variable robin coefficient, Comput. Methods Appl. Mech. Eng. 198 (41–44) (2009) 3187–3206.
[4] A. Ammar, B. Mokdada, F. Chinesta, R. Keunings, A new family of solvers for some classes of multidimensional partial differential equations encountered in kinetic theory modeling of complex fluids, J. Non-Newton. Fluid Mech. 139 (2006) 153–176.
[5] J. Artwell, B. King, Proper orthogonal decomposition for reduced basis feedback controllers for parabolic equations, Math. Comput. Model. 33 (1–3) (2001) 1–19.
[6] L. Machiels, Y. Maday, A. Patera, Output bounds for reduced-order approximations of elliptic partial differential equations, Comput. Methods Appl. Mech. Eng. 190 (2001) 3413–3426.
[7] M.A. Grepl, A.T. Patera, A posteriori error bounds for reduced-basis approximations of parametrized parabolic partial differential equations, Model. Math. Anal. Numer. 39 (1) (2005) 157–181.
[8] D. Rovas, L. Machiels, Y. Maday, Reduced-basis output bound methods for parabolic problems, IMA J. Numer. Anal. 26 (3) (2006) 423–445.
[9] P. Kerfriden, J.J. Rodenas, S.P.A. Bordas, Certification of projection-based reduced order modeling in computational homogenization by the constitutive relation error, Int. J. Numer. Methods Eng. 97 (6) (2014) 395–422.
[10] E. Florentin, P. Díez, Adaptive reduced basis strategy based on goal oriented error assessment for stochastic problems, Comput. Methods Appl. Mech. Eng. 225-228 (2012) 116–127.
[11] P. Ladevèze, D. Leguillon, Error estimate procedure in the finite element method and application, SIAM J. Numer. Anal. 20 (3) (1983) 485–509.
[12] P. Ladevèze, L. Chamoin, On the verification of model reduction methods based on the proper generalized decomposition, Comput. Methods Appl. Mech. Eng. 200 (2011) 2032–2047.
[13] J.P.M. de Almeida, A basis for bounding the errors of proper generalized decomposition in solids mechanics, Int. J. Numer. Methods Eng. 94 (2013) 961–984.
[14] L. Gallimard, P. Ladevèze, J. Pelle, Error estimation and adaptivity in elastoplasticity, Int. J. Numer. Methods Eng. 39 (1996) 189–217.
[15] P. Ladevèze, N. Moës, A new a posteriori error estimation for nonlinear time-dependent finite element analysis, Comput. Methods Appl. Mech. Eng. 157 (1997) 45–68.
[16] J. Pelle, D. Ryckelynck, An efficient adaptive strategy to master the global quality of viscoplastic analysis, Comput. Struct. 78 (2000) 169–183.
[17] L. Gallimard, T. Sassi, A posteriori error analysis of a domain decomposition algorithm for unilateral contact problem, Comput. Struct. 88 (13–14) (2010) 879–888. http://dx.doi.org/10.1016/j.compstruc.2010.04.007.
[18] V. Rey, C. Rey, P. Gosselet, A strict error bound with separated contributions of the discretization and of the iterative solver in non-overlapping domain decomposition methods, Comput. Methods Appl. Mech. Eng. 270 (0) (2014) 293–303. http://dx.doi.org/10.1016/j.cma.2013.12.001.
[19] P. Ladevèze, J. Pelle, P. Rougeot, Error estimation and mesh optimization for classical finite elements, Eng. Comput. 8 (1991) 69–80.
[20] L. Gallimard, A constitutive relation error estimator based on traction-free recovery of the equilibrated stress, Int. J. Numer. Methods Eng. 78 (2009) 460–482.
[21] P. Ladevèze, L. Chamoin, E. Florentin, A new non-intrusive technique for the construction of admissible stress fields in model verification, Comput. Methods Appl. Mech. Eng. 199 (9–12) (2010) 766–777. http://dx.doi.org/10.1016/j.cma.2009.11.007.
[22] L. Gallimard, P. Ladevèze, J. Pelle, Error estimation and time-space parameters optimization for fem non-linear computation, Comput. Struct. 64 (1997) 145–156.
[23] P. Ladevèze, N. Moës, Adaptive control for finite element analysis in plasticity, Comput. Struct. 73 (1999) 45–60.
[24] J. Peraire, A. Patera, Bounds for linear-functional outputs of coercive partial differential equations: local indicators and adaptive refinement, in: P. Ladevèze, J. Oden (Eds.), Advances in Adaptive Computational Methods, Elsevier, 1998, pp. 199–216.